8.1-THz Displacement-field Nano-switches for 5G and beyond

M. Samizadeh Nikoo*, T. Wang, P. Sohi, M. Zhu, F. Qaderi, R. A. Khadar, A. Floriduz, A. M. Ionescu, and E. Matioli*
EPFL, CH-1015 Lausanne, Switzerland, *email: mohammad.samizadeh@epfl.ch; elison.matioli@epfl.ch

***Abstract*—**The rapid progress in high capacity communication systems is reaching extremely high data rates of 100 Gb s^{-1}, which demands electronic switches with cut-off frequencies well above 1 THz. The excellent electron transport properties of III-V heterojunctions could potentially enable terahertz devices, however, the high parasitic capacitances and contact resistances in traditional ultra-scaled electronic devices, such as transistors and diodes, hinder their potential. Here we demonstrate that the fast switching of displacement fields strongly confined in a few-nanometers-thin crystal between a textured metal and an electron sheet, so called displacement-field nano-switch, can provide cut-off frequencies above 8 THz, enabling an efficient switching of terahertz signals. The device offers extremely low ON state resistances approaching 100 Ω μm, low parasitic capacitances in range of 100 aF μm^{-1}, excellent impedance matching capability, and fast switching times down to 10 ps. We demonstrate the application of these devices for high data rate modulation and mixing. The outstanding performance and integration capability of displacement-field nano-switches pave the way towards mm-wave and terahertz integrated circuits with applications in 5G and 6G communications, among others.

I. Introduction

Terahertz is a key technology for a wide range of applications, from security and imaging to fundamental sciences [1], [2]. The sixth generation of telecommunications and beyond will be operating at ultrahigh data rates that can reach 100 gigabits per second, requiring efficient and robust terahertz switches for data modulation [3]. Conventional electronic and optical devices, however, fail to operate efficiently at this frequency range, which defines a so-called terahertz gap [4]. This significantly hinders the development of the next generation of radiofrequency systems, highlighting the need for new ultrahigh speed devices to bridge the spectrum gap between microwave and optical frequencies.

The evolution of high-speed conventional electronic devices has relied on an extreme shrinkage of the device dimensions, which, as a consequence increases the relative weight of the parasitic components on the device performance. This trade-off poses a limit on the effectiveness of further scaling. The performance of ultra-scaled devices is hindered by the tunneling through contacts and high parasitic capacitances. Schottky barrier diodes with regrown contacts [5] are the fastest electronic device up to date, presenting cut-off frequencies of about 3 THz in wafer scale [6]. In this work, we demonstrate that the excellent field coupling between a micro-textured metal and a two-dimensional electron gas (2DEG), a few nanometers apart from each other, provides an excellent metal-semiconductor contact, breaking the trade-off between ON resistance (R_{ON}) and OFF capacitance (C_{OFF}). We demonstrate devices with R_{ON} approaching 100 Ω·μm, cut-off frequencies beyond 8 THz, and excellent dynamic performance with a switching time down to 10 ps. These results make them an outstanding candidate for future high speed electronics.

II. Device Concept

Fig. 1a shows a schematic of a displacement-field nano-switch including a nano-gap formed by two identically-shaped metallic pads on a high-electron-mobility heterojunction with a thin barrier. At direct-current (dc) regime, the device provides isolation between the two ports, so no static power is dissipated. A high-frequency signal, however, can be transmitted from one port to another, thanks to the strong electric-field coupling between the metal and the floating 2DEG. We show that this coupling is drastically enhanced by replacing the simple straight-edge pads by a microstructured metal, leading to an outstandingly low resistance with very small parasitics. By applying a control signal to one of the ports, the 2DEG at the interface is depleted, eliminating the electric-field coupling, which turns OFF the switch. The simple and self-aligned fabrication in which the entire device is patterned in a single lithography step enables ultra-scaling the channel length to below 50 nm (Fig. 1b). Fig. 1c shows the channel impedance during a switching event in a conventional field-effect transistors (FETs) and diodes (red line) and in a displacement-field nano-switch (blue line). Traditional devices switch ohmic currents along the real axis. Alternatively, displacement-field nano-switch switch displacement currents along the imaginary axis. Fig. 1d presents the measured channel impedance of a displacement-field nano-switch for different bias voltages, indicating three orders of magnitude switching in the imaginary component of the impedance. The switch can be also implemented as a three-port device by adding a gate electrode, either as a back-gate (Fig. 1e), or as a typical top-gate between the two contacts.

III. Results and Discussions

The scattering (*S*) parameters of displacement-field nano-switches fabricated on two different epitaxies were measured using a vector network analyzer (VNA) (Fig. 2a). Epitaxy A is composed of InAlN/GaN with a 7.5-nm-thin barrier, and epitaxy B has an AlGaN/GaN heterostructure with a 27-nm-thin barrier. In both cases, Au (50 nm)/Ni (50nm) contacts with 320 nm-long gap were used. Both epitaxies present almost identical sheet resistance of ~300 Ω/□, however, the thin-barrier epitaxy (A) yields a much lower insertion loss, indicating the superior

metal-2DEG coupling (Fig. 2b). This shows the critical role of field confinement in the barrier, which can be explained based on the distributed circuit model (Fig. 2c). A stronger field confinement, which can be achieved with thinner barriers or at higher frequencies, results in a smaller barrier reactance, thus concentrating the current density closer to the gap (Fig. 2c). This effectively reduces the impact of ohmic resistance of metals on the device resistance. Based on the *S* parameters, we extracted the R_{ON} of devices with different gap lengths fabricated on epitaxy A, up to 110 GHz (Fig. 3a). These results show the reduction of R_{ON} for smaller gaps and as the frequency increases due to the smaller barrier reactance, reaching values below 200 Ω·μm at 110 GHz. From these measurements, an effective contact resistance of R_C = 80 Ω·μm at 100 GHz was extracted from transfer length method (TLM) (Fig. 3b).

Designing displacement-field devices with multiple narrow fingers (microstructured devices), with similar gap length, can drastically change the current density distribution and enhance the device performance by breaking the trade-off between R_{ON} and C_{OFF}. Figs. 4a and 4b show the two geometries of displacement-field switches presented in this work. The normalized R_{ON} and C_{OFF} measured at 50 GHz (Figs. 4c and 4d, respectively) reveal that the multi-finger devices exhibit more than two times lower resistance, and about two times lower capacitance compared to the straight-gap device. We note that the entire width of the gap in the multi-finger structure was considered in the normalization, although the $R_{ON}C_{OFF}$ product, which is 4 times lower in the multi-finger devices, is a self-normalized parameter and clearly shows the superior performance of multi finger devices. While a cut-off frequency ($f_c = 1/2\pi R_{ON}C_{OFF}$) of 1.5 THz was obtained for 220-nm-long straight-gap devices, multi-finger devices with the same gap length presented an outstandingly higher value of 6.2 THz. The R_{ON} of multi finger devices further decreases at higher frequencies, reaching an ultralow value of 120 Ω·μm at 100 GHz (Fig. 5), corresponding to a cut-off frequency of 8.1 THz. The extreme field confinement, and the multi finger device geometry, drastically boosted the performance of displacement-field nano-switches with respect to previous capacitively-coupled contacts [7], such as metal-2DEG-metal varactors [8], which provide cut-off frequencies below 2 THz. The ultralow resistance of microstructured metal to a semiconductor can be a universal approach, offering an alternative to nonalloyed or semi-metal contacts at high frequencies [9]-[11].

Fig. 6 benchmarks the R_{ON} and C_{OFF} obtained for multi finger displacement-field nano-switches fabricated on epitaxies A (solid star) and B (hollow star). The proposed devices are no longer limited by the metal-semiconductor tunneling resistance, and thanks to their high conductance and low parasitic capacitance, exhibit cut-off frequencies much higher than conventional devices such as diodes and transistors. Such a superior performance offer great prospects for high speed electronics with applications in high data-rate signal modulation and mixing, as presented in the following section.

Displacement-field nano-switches also exhibit a promising matching capability without requiring extra matching networks. Figs. 7a and 7b show the transmission and reflection of a multi finger switch. The device exhibits a 0.6 dB insertion loss and ON/OFF ratio of 10 dB at 110 GHz, and provides a good matching in a very wide frequency range from 30 GHz to 110 GHz. The range of impedance matching can be easily tuned by a layout design (Fig. 6c).

IV. High-data Rate Modulation

In addition to the low insertion loss and high isolation, displacement-field nano-switches also provide an excellent dynamic performance and show ultrafast switching between ON and OFF states, which enable ultrahigh-speed data transmission. Figs. 8a and 8b show the experimental set-up to demonstrate the dynamic behavior of the proposed devices. A local oscillator (LO) generates a carrier signal, which is combined with a base-band data signal, and applied to one port of a displacement-field nano-switch. The switch was biased close to the threshold voltage, at 3.5 V (Fig. 1d). The second terminal was terminated by a 50-Ω port of a 70-GHz oscilloscope, to measure the modulated signal.

To show the signal modulation at high data rates, we employed a continuous wave sinusoidal signal as the data signal. Fig. 8c shows the modulated signal with a 50-GHz carrier, and the calculated spontaneous power of the signal is shown in Fig. 8d. These results reveal a 6 Gb s^{-1} data modulation with an ON/OFF switching well below 100 ps. Fig. 8e presents the fast Fourier transform (FFT) of the modulated signal presented in Fig. 8c, which shows an excellent multiplication with three pronounced side harmonics. Displacement-field nano-switches are also excellent candidates for mixing applications. Fig. 8f shows mixing a 15-GHz large signal LO with a 50-GHz RF signal, indicating a very fast dynamic performance, with a switching time down to 10 ps.

V. Conclusion

Displacement-field nano-switches provide an excellent coupling between a textured metallic contact and a 2DEG, breaking the trade-off between R_{ON} and C_{OFF}. We demonstrated that this device concept with a relatively long channel length (> 200 nm) enables an ultralow total R_{ON} of 120 Ω·μm along with extremely high cut-off frequencies beyond 8 THz. The devices are compatible with common planar fabrication methods and can be integrated on III-V platforms as part of the future high-speed electronic circuits. The simplicity and high performance of the proposed devices pave the way toward high frequency integrated systems, with application in 5G, 6G, among others.

References

[1] K. Sengupta, T. Nagatsuma, and D. M. Mittleman, *Nature Electron.* 1, 622–635, 2018.
[2] T. S. Rappaport *et al.*, *IEEE Access* 7, 78729–57, 2019.
[3] S. Dang, *et al. Nat. Electron.* 3, 20–29, 2020.
[4] M. Tonouchi, *Nat. Photon.* 1, 97–105, 2007.
[5] K. Shinohara *et al. IEEE Trans. Electron Devices* 60, 2982–2996, 2013.
[6] B. T. Bulcha *et al. IEEE Trans. THz Sci. Technol.* 6, 737–746, 2016.
[7] A. Koudymov *et al. IEEE Electron Device Lett.* 30, 478–480, 2009.
[8] J. H. Hwang *et al. IEEE Electron Device Lett.* 40, 1740-1743, 2019.
[9] K. J. Chen, *et al. IEEE Trans. Electron Devices*. 43, 252–257, 1996.
[10] S. Dasgupta, *et al. Appl. Phys. Lett.* 96, 143504, 2010.
[11] P.-C. Shen, *et al.*, *Nature* 593, 211–217, 2021.

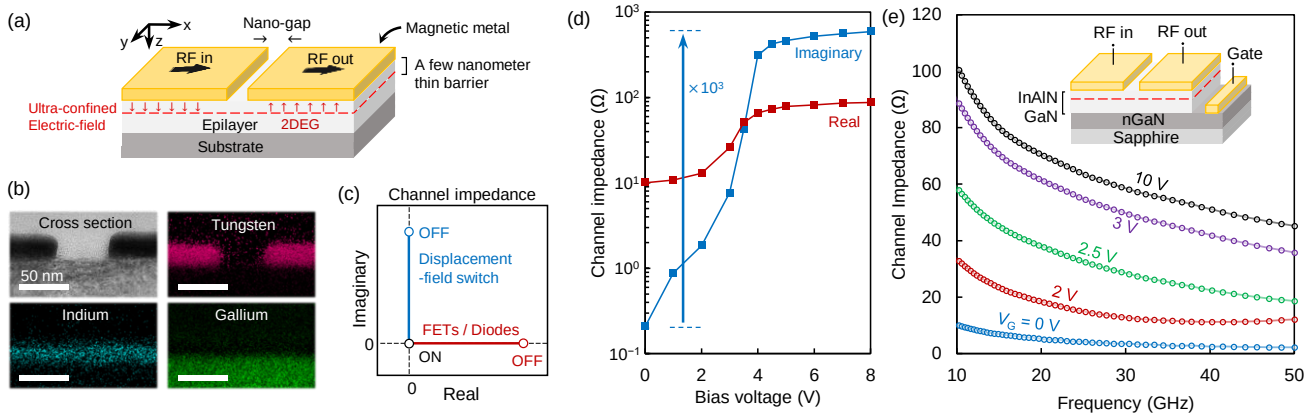

Fig. 1. (a) Simplified structure of a displacement-field nano-switch realized on a high-electron-mobility heterostructure with a few-nanometer thin barrier. (b) Transmission electron microscopy (TEM) image of an ultra-scaled displacement-field nano-switch with a 50-nm gap distance, together with energy-dispersive X-ray (EDX) spectroscopy for Tungsten (metallic pads), Indium, and Gallium. (c) The channel impedance in diodes and field-effect transistors lies in the real axis, while a displacement-field switch relies on the modulation of the imaginary part of the impedance. (d) Measured channel impedance (real and imaginary parts) for a displacement field nano-switch showing three orders of magnitude switching in the imaginary part of the channel impedance. (e) Implementation of a three-port displacement-field nano-switch with a back gate realized by a 600-nm-thick epitaxially grown highly doped (1×10^{19} cm^{-3}) GaN layer. The results show 20 times change in impedance at 50 GHz corresponding to a 26 dB switching.

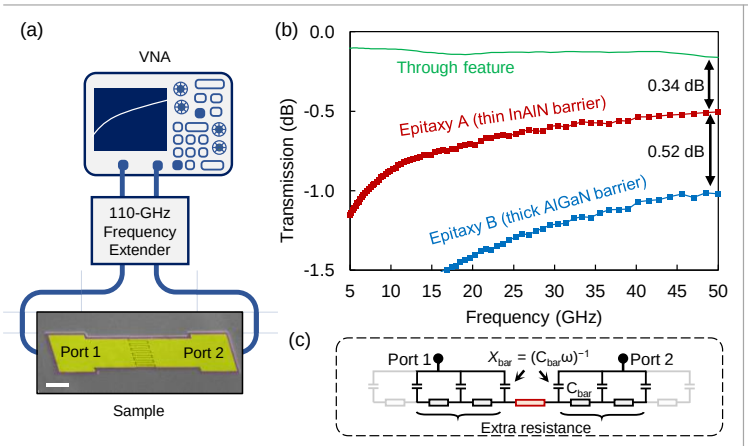

Fig. 2. (a) Experimental setup to evaluate signal transmission through metal-2DEG coupling. The SEM image shows a 300-nm-long-gap device. Scale bar is 10 µm. (b) Transmission scattering parameter of a 7.5-nm-thin barrier based on InAlN and a 27-nm-thin barrier based on AlGaN, both providing $R_{sh} \sim 300$ Ω/□. With respect to the through feature (short circuit of input and output terminals), the thin-barrier provide a 2.5-times lower insertion loss. (c) A circuit model based on distributed capacitance-resistances indicates a higher performance for ultrathin barrier epitaxies, as the metal-2DEG coupling enhances due to a lower barrier reactance X_{bar}.

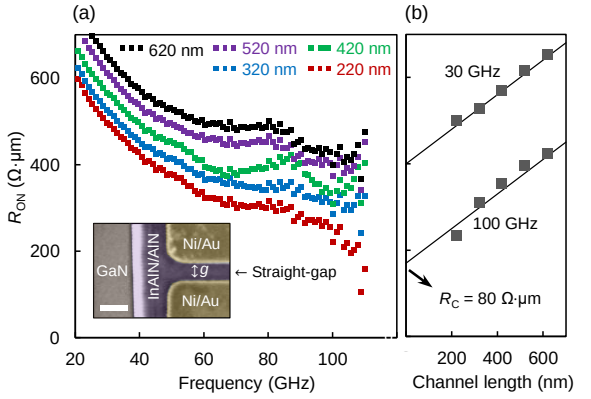

Fig. 3. (a) ON-state resistance of displacement field nano- switches with straight-gap distances g = 220 nm, 320 nm, 420 nm, 520 nm, and 620 nm. The total resistance of 220-nm-long channel devices reaches 200 Ω.µm at frequencies above 100 GHz. The inset shows the SEM image of a switch. The scale bar is 300 nm. (b) The extracted effective contact resistance of the devices using TLM at radiofrequencies. Measurements at 30 GHz and 100 GHz show almost identical sheet resistance, however, the contact resistance drops at higher frequencies thanks to a stronger metal-2DEG coupling.

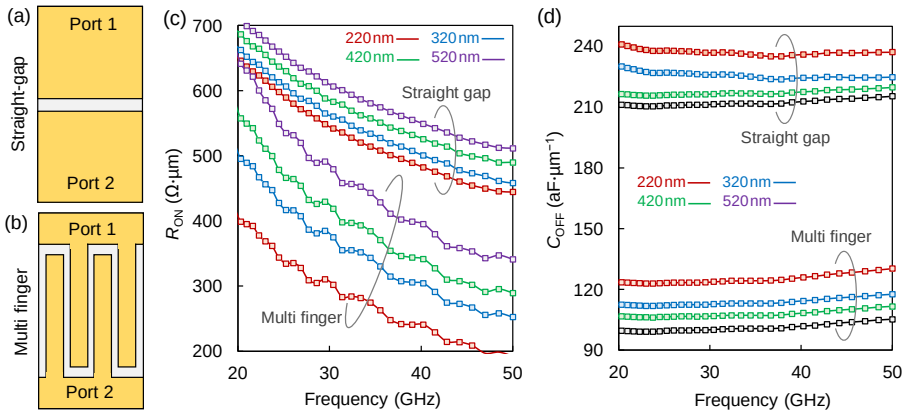

Fig. 4. Comparison of ON and OFF states of devices with (a) straight-gaps and (b) multi finger pads in which the devices consist of 1.2-µm-wide 10-µm-long fingers, with the same gap length g. (c), (d) Normalized R_{ON} and C_{OFF} of straight-gap devices for different gap lengths. 220-nm-long gap devices exhibit R_{ON} = 444 Ω·µm and C_{OFF} = 237 aF·µm^{-1} at 50 GHz resulting in a 1.5 THz cut-off frequency. (e), (f) Normalized R_{ON} and C_{OFF} of microstructured devices with 16 fingers for different gap lengths. 220-nm-long gap devices exhibit R_{ON} = 197 Ω·µm and C_{OFF} = 130 aF·µm^{-1} at 50 GHz resulting in a 6.2 THz cut-off frequency. These results indicate a lower resistance and a lower capacitance for multi finger devices.

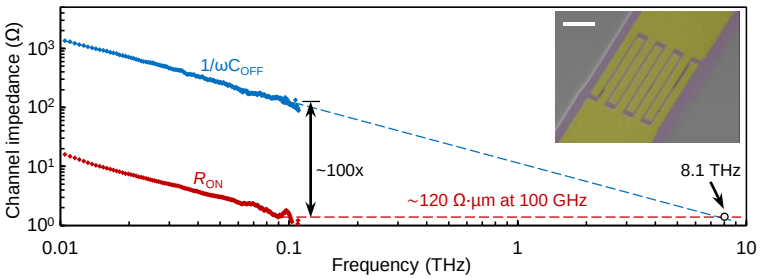

Fig. 5. The channel impedance corresponding to the OFF state capacitance and ON state resistance for the microstructure device shown in the inset (the scale bar is 4 μm). Measurements at 100 GHz shows an 8.1 THz cut-off frequency.

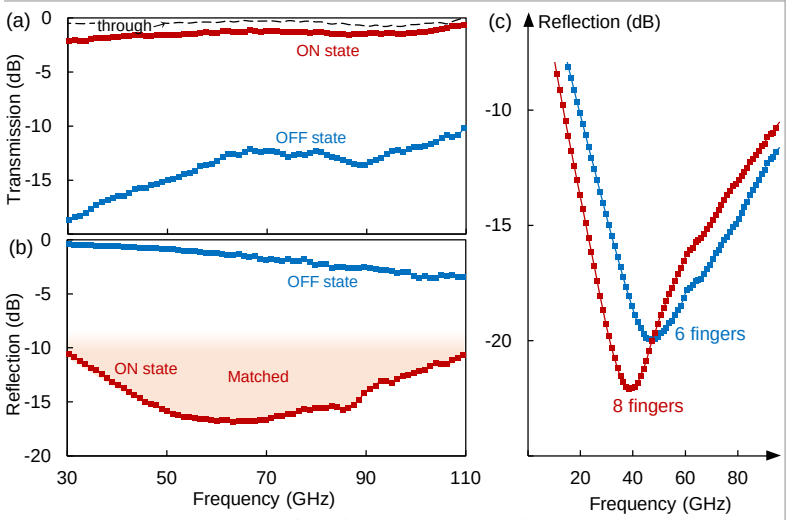

Fig. 7. Scattering parameters of a 4-finger displacement-field nano-switch in ON and OFF states. (a) Transmission (S_{21}). (b) Reflection (S_{11}). The switch exhibits a low insertion loss < 1 dB at 100 GHz with over 10 dB isolation. (c) The device geometry such as number of fingers can tune the matched frequency band.

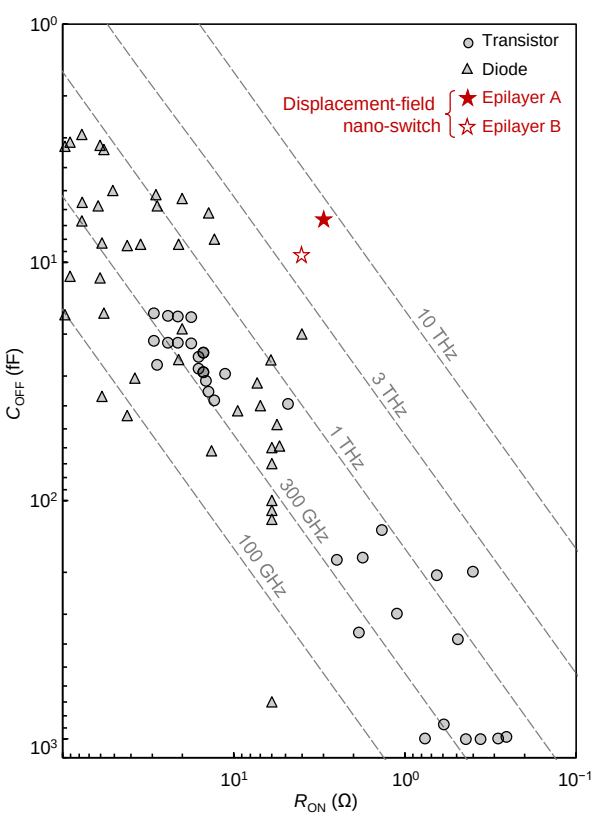

Fig. 6. Benchmark of multi finger displacement-field nano-switches fabricated on epitaxy A (InAlN/AlN/GaN with a thin barrier) and epitaxy B (AlGaN/GaN with a thick barrier). The devices exhibit a superior performance comparing to traditional electronic devices such as transistors and diodes.

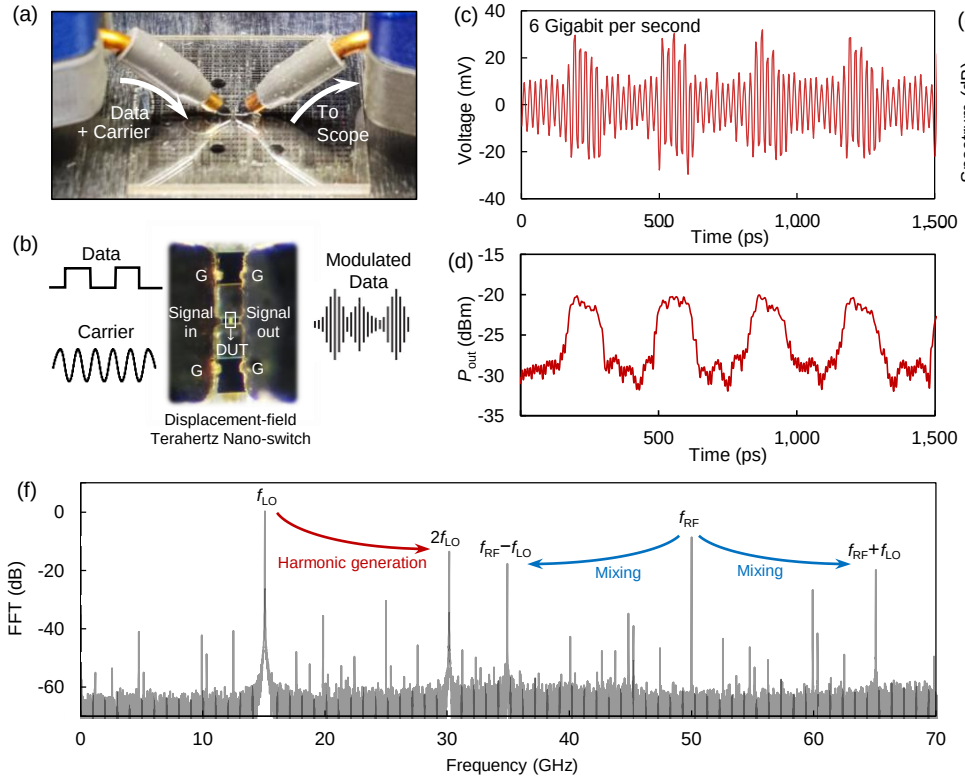

Fig. 8. (a) Experimental setup in which one port of the switch is excited by carrier and data signal (after a power combiner) and the second port is terminated by the 50-Ω port of a 70-GHz scope. (b) Photograph of the switch connected to radiofrequency GSG probes for measurements up to 67 GHz. (c) Ultrahigh speed data transmission with a 50-GHz carrier and a sinusoidal signal as the data source, resulting in a 6 Gb s^{-1} data transmission. (d) Instantaneous power corresponding to the waveform shown in part c. (e) FFT of the modulated signal. (f) Displacement field switches for mixing and second harmonic generation, using a 15 GHz LO and 50 GHz RF signals.